



1           **A Novel Methodology for Assessing the Hygroscopicity of Aerosol Filter Samples**

2                           **Nagendra Raparathi<sup>1</sup>, Anthony S. Wexler<sup>1,2,3,4</sup>, Ann M. Dillner<sup>1</sup>**

3                           <sup>1</sup>Air Quality Research Center, University of California, Davis, 95616 CA, USA

4                           <sup>2</sup>Mechanical and Aerospace Engineering, University of California, Davis, 95616 CA, USA

5                           <sup>3</sup>Civil and Environmental Engineering, University of California, Davis, 95616 CA, USA

6                           <sup>4</sup>Land, Air, and Water Resources, University of California, Davis, 95616 CA, USA

7

8                           *Correspondence to:* Ann M. Dillner ([amdillner@ucdavis.edu](mailto:amdillner@ucdavis.edu))

9

10

11

12

13

14

15

16

17

18

19

20

21

22

23

24

25



26 **Abstract**

27 Due to US regulations, concentrations of hygroscopic inorganic sulfate and nitrate have declined  
28 in recent years, leading to an increased importance in the hygroscopic nature of organic matter  
29 (OM). The hygroscopicity of OM is poorly characterized because only a fraction of the multitude  
30 of organic compounds in the atmosphere are readily measured and there is limited information on  
31 their hygroscopic behaviours. Hygroscopicity of aerosol is traditionally measured using  
32 Humidified Tandem Differential Mobility Analyzer (HTDMA) or Electrodynamic Balance  
33 (EDB). EDB measures water uptake by a single particle. For ambient and chamber studies,  
34 HTDMA measurements provide water uptake and particle size information but not chemical  
35 composition. To fill in this information gap, we have developed a novel methodology to assess  
36 the water uptake of particle collected on Teflon filters, thereby providing an opportunity to link  
37 the measured hygroscopicity with ambient particle composition. To test the method, hygroscopic  
38 measurements were conducted in the laboratory for ammonium sulfate, sodium chloride, glucose,  
39 and malonic acid, which were collected on 25mm Teflon filters using an aerosol generator and  
40 sampler. Constant humidity solutions (CHS) were employed to maintain the relative humidity  
41 (RH) at approximately 84%, 90%, and 97% in small chambers. Hygroscopic parameters, including  
42 the water-to-solute (W/S) ratio, molality, mass fraction solute (mfs), and growth factors (GF), were  
43 calculated from the measurements. The results obtained are consistent with those reported by the  
44 E-AIM model and previous studies utilizing HTDMA and EDB for these compounds, highlighting  
45 the accuracy of this new methodology. This new approach enables the hygroscopicity and  
46 chemical composition of individual filter samples to be assessed so that in complex mixtures such  
47 as chamber and ambient samples, the total water uptake can be parsed between the inorganic and  
48 organic components of the aerosol.

49 **Keywords:** Hygroscopicity, Organic Aerosol, Teflon Filters, Constant Humidity Solutions

50

51

52

53

54



55 **Highlights**

- 56       • This is the first study to assess the hygroscopicity of particles collected on Teflon filters.
- 57       • This study's methodology can evaluate water uptake at RH levels as high as ~97%.
- 58       • This methodology enables the investigation of composition-dependent hygroscopicity of
- 59       particles.

60

61

62

63

64

65

66

67

68

69

70

71

72

73

74

75

76

77

78



## 79 1. Introduction

80 Atmospheric particles significantly degrade air quality by reducing visibility and posing health  
81 risks to humans (Gupta et al., 2022; Kohli et al., 2023; Qu et al., 2020). Additionally, they function  
82 as cloud condensation nuclei (CCN) or ice-nucleating particles (INPs), profoundly influencing  
83 cloud properties and consequently exerting a significant effect on Earth's radiation budget (Haseeb  
84 et al., 2024; Lee et al., 2008; Li et al., 2022; Mikhailov et al., 2021; Nadler et al., 2019; Reich et  
85 al., 2023; Sjogren et al., 2007; K. Wang et al., 2021; Zieger et al., 2017). Atmospheric aerosol  
86 consists of both organic and inorganic compounds with varying physicochemical properties, which  
87 further determine the CCN activity, reactivity, deposition, and optical properties (Padró et al.,  
88 2012; J. Wang et al., 2010). Historically, the hygroscopic (water-attracting) characteristics of CCN  
89 were primarily influenced by inorganic compounds such as nitrates, sulfates, and chlorides.  
90 However, with the implementation of emissions controls that have successfully reduced nitrogen  
91 and sulfur oxide emissions, the organic fraction of aerosol is assuming a more prominent role.  
92 Additionally, the organic fraction is considerably more complex than its inorganic counterpart,  
93 comprising thousands of individual compounds originating from diverse sources and reaction  
94 pathways, each possessing distinct physical and chemical properties (Boris et al., 2019; Jathar et  
95 al., 2016). This complexity often poses challenges to establishing a clear correlation between the  
96 organic fraction and hygroscopicity (Han et al., 2022).

97 The hygroscopicity of particles, which refers to their ability to absorb water, depends on both size  
98 and chemical composition (Luo et al., 2020; Zieger et al., 2017). The water activity of atmospheric  
99 particles, particularly the affinity of various solutes for water, plays a crucial role in governing  
100 several important factors. These include the “total mass concentration of airborne particles, their  
101 acidity, the extent of light scattering, their rates of aqueous phase chemical reactions, and their  
102 ability to act as cloud condensation nuclei (CCN)” (Saxena et al., 1995). To characterize these  
103 attributes of airborne particles, it is necessary to know the amount of water uptake as a function of  
104 particle composition and relative humidity (RH) (Saxena et al., 1995).

105 Various thermodynamic models are available for estimating hygroscopicity, including,  
106 ISORROPIA (Nenes et al., 1998), Aerosol Inorganic-Organic Mixtures Functional groups Activity  
107 Coefficients (AIOMFAC) (Zuend et al., 2010), Extended Aerosol Inorganic Model (E-AIM)  
108 (Clegg et al., 1998), Universal Quasi-Chemical Functional group Activity Coefficients (UNIFAC)



109 model (Fredenslund et al., 1975), and the University of Manchester System Properties  
110 (UManSysProp) (Topping et al., 2016). For the organics, they utilize group contribution methods  
111 to estimate the water activity of ambient species relevant to the atmosphere (Han et al., 2022).  
112 However, these models require further experimental data to validate them and refine their  
113 predictions (Han et al., 2022).

114 Previous studies have measured the hygroscopic growth of both inorganic and organic compounds  
115 relevant to the atmosphere. Techniques such as the Humidifier Tandem Differential Mobility  
116 Analyzer (HTDMA) (Boreddy et al., 2014; Laskina et al., 2015; Mikhailov et al., 2021) and the  
117 Electrodynamic Balance (EDB) (Chan et al., 1992, 2000; Cohen et al., 1987; Kohli et al., 2023;  
118 Peng et al., 2001; Steimer et al., 2015; Tang & Munkelwitz, 1991) have been utilized for this  
119 purpose. EDB measures the change in mass of individual charged particles of known composition,  
120 which are levitated in a gaseous atmosphere by means of an electric field created by imposing  
121 voltages on the electrodes (Cohen et al., 1987; Kohli et al., 2023). When the mass of a levitating  
122 particle undergoes evaporation or condensation due to a change in RH, it becomes proportional to  
123 the DC voltage required to balance the particle in a stationary position. The particle's mfs can then  
124 be determined by measuring the particle's balancing voltage with that of a reference state of known  
125 composition (Peng et al., 2001). However, EDB is limited to analyzing single particles and is not  
126 suitable for studying the water uptake of ambient samples. HTDMA measures the change in  
127 particle size distribution in response to varying humidity levels and can be used to measure ambient  
128 aerosol. By exposing aerosol particles to controlled humidity levels and measuring their sizes  
129 before and after exposure, HTDMA assesses the extent of hygroscopic growth as a function of  
130 particle size. This method measures the change in the diameter of the particles, from which  
131 parameters such as mass fraction of the solute (mfs) and solute molality are estimated. However,  
132 this method does not measure chemical composition of the particles and faces challenges in  
133 measuring RH conditions exceeding 90% (Marsh et al., 2019), an RH regime that can lead to very  
134 high water uptake. Therefore, there is a need to devise a laboratory technique capable of measuring  
135 composition-dependent water uptake of aerosol sampled on the Teflon filters.

136 This study's objective is to devise a methodology for assessing the water uptake of organic and  
137 inorganic aerosol collected on Teflon filters which are commonly used for gravimetric and  
138 chemical analysis. Our aim is to accurately estimate water adsorption by solute molecules that



139 commonly act as cloud condensation nuclei (CCN), which include atmospheric relevant inorganics  
140 such as ammonium sulfate and sodium chloride, as well as organics such as glucose, a sugar, and  
141 malonic acid, a dicarboxylic acid. We compare the results obtained to data from the literature to  
142 gain insights into the accuracy of the methodology developed. The novelty of this research lies in  
143 the development of method to determine the hygroscopicity of aerosol filter samples so that the  
144 chemical composition can be measured and to measure at high relative humidity, exceeding 90%,  
145 which is relevant to CCN and where most organic and inorganic compounds absorb considerable  
146 amounts of water.

## 147 **2. Experimental observations**

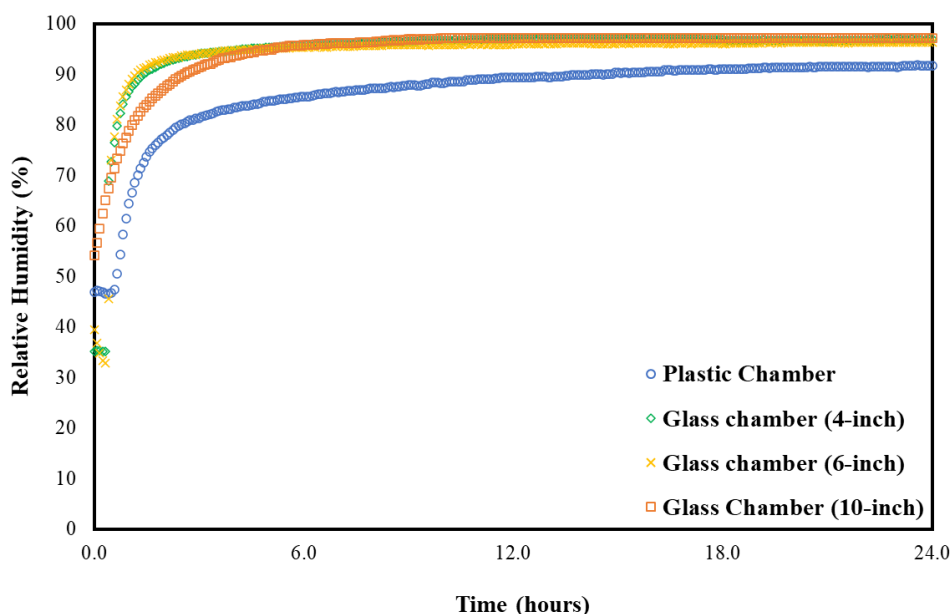
### 148 **2.1. Relative Humidity Controlled Chamber**

149 The initial step in developing this methodology involves maintaining RH throughout the  
150 entire water uptake measurement process. Constant humidity solutions (CHS) (Lide, 2004) offer  
151 a means to sustain specified RH levels within sealed chambers. In this study, our aim was to  
152 measure the water uptake of both organic and inorganic compounds across a range of high RH  
153 levels above 80%. Potassium chloride, barium chloride dihydrate, and potassium sulfate were  
154 selected for their capacity to maintain RH levels of approximately 84%, 90%, and 97%,  
155 respectively, in their saturated form. Prior to conducting the actual water uptake measurements,  
156 we placed these saturated solutions in 10-inch plastic and glass chambers for 24 hours to assess  
157 their practical efficacy. In addition, a real-time RH and temperature sensor (Rotronic HL-1D, with  
158 an accuracy of  $\pm 3.0\%$  RH and  $\pm 0.3^{\circ}\text{C}$ ) was placed inside the chambers. In the glass chambers, the  
159 RH reached the desired RH levels, but not so in the plastic chambers, likely due to the absorption  
160 by the plastic itself (Fig. 1). Wexler and Hasegawa (1954) specifically noted that chambers should  
161 be made of non-hygroscopic materials, preferably metal or glass, as otherwise, the time required  
162 to achieve RH equilibrium could be substantial, sometimes spanning days or weeks. Similar  
163 observations were made in our study.

164 Next, we used 4, 6, and 10-inch diameter glass chambers, to examine the consistency of  
165 RH levels across different chamber sizes. As expected, all these chambers reached their optimal  
166 RH depending on the saturated solutions used but there was a difference in time to equilibration.  
167 For instance, the initial time taken to reach the desired RH of  $\sim 97\%$  (saturated  $\text{K}_2\text{SO}_4$ ) for a 10-  
168 inch chamber was slightly longer compared to 4- and 6-inch chambers (Fig. 1). Based on these



169 observations, it is evident that RH equilibrium is influenced by the presence of hygroscopic  
 170 materials, and the ratio of the solution’s free surface area to the chamber volume. These findings  
 171 affirm the appropriateness of CHS for conducting water uptake measurements using glass  
 172 chambers of any size and that smaller sizes equilibrate more quickly.  
 173



174 **Figure 1.** RH over 24-hours in the plastic (10-inch) and glass (4, 6, and 10-inch) chamber  
 175 with saturated K<sub>2</sub>SO<sub>4</sub> solution  
 176  
 177

178 **2.1.1. Determining the RH (a<sub>w</sub>) for the CHS**

179 In the CRC Handbook (volume 85), (Lide, 2004) provided integer RH values for CHS at  
 180 25<sup>0</sup>C. However, even a small variation in RH could substantially affect water uptake, particularly  
 181 at higher RH levels, where the water uptake change per change in RH is very steep. The average  
 182 temperature during these experiments ranged from 17.9<sup>0</sup>C to 21.6<sup>0</sup>C. To evaluate the effect of  
 183 temperature variation on RH, the water activity over this range was calculated for each compound  
 184 used to create CHS. The water activity is ~0.843 for saturated KCl and ~0.975 for saturated K<sub>2</sub>SO<sub>4</sub>,  
 185 with no significant variation within the temperature range, according to Eq. (1) provided by Wexler  
 186 & Seinfeld (1991),

187 
$$\ln \frac{a_w(T)}{a_w(T_0)} = -\frac{M_w}{1000} m_s \frac{L_s}{R} \left( \frac{1}{T} - \frac{1}{T_0} \right) \quad (1)$$



188 where  $a_w(T)$  is the water activity at temperature (T),  $a_w(T_0)$  is the water activity at temperature  
189 ( $T_0$ , 298.15K),  $M_w$  is the molecular weight of water (18.01528 g/mol),  $m_s$  is the saturated molality  
190 of the compound used as CHS, R is the universal gas constant (8.314 kJ/kmol-K) and  $L_s$  is the  
191 latent heat of fusion for the salt from a saturated solution; it equals the difference between the  
192 standard heat of formation of the crystalline solid phase ( $\Delta H_{f,c}$ ) and ( $\Delta H_{f,aq}$ ), the standard heat of  
193 formation of the species in the aqueous solution at saturation molality. For  $a_w(T_0)$ , the values are  
194 0.8426 for KCl and 0.975097 for  $K_2SO_4$  (Kim & Seinfeld, 1995). The average saturated molality  
195 ( $m_s$ , in mol/kg) is 4.604 for KCl (Shearman & Menzis, 1937) and 0.636 for  $K_2SO_4$  (Krumgalz,  
196 2018). The latent heat of fusion ( $L_s$ , in kJ/mol) is -15.287 for KCl and -23.77 for  $K_2SO_4$  (Kim &  
197 Seinfeld, 1995).

198 The water activity for saturated  $BaCl_2 \cdot 2H_2O$  was determined by extrapolating the water activities  
199 provided by (X. Wang et al., 2013) at temperatures of 5, 15, 25, and 35°C (See Fig. S1). The  
200 average  $a_w$  for saturated  $BaCl_2 \cdot 2H_2O$  during these experiments was ~0.908, ranging from 0.906 to  
201 0.911 and for each experiment the variability in RH due to temperature fluctuations in the lab was  
202 negligible (less than 0.25%).

203

## 204 **2.2. Laboratory sample collection**

205 The laboratory particulate samples were produced utilizing a home-built aerosol generator  
206 and sampler, which consists of an atomizer (Aerosol generator 3076, TSI Inc., USA), a custom-  
207 built diffusion dryer, and an IMPROVE aerosol sampler operated at 22.8 L/min. The aerosol  
208 generator and sampler was used to generate and collect the known mass of each target compound  
209 onto 25 mm Teflon filters (MTL, USA). De-ionized water (~18.2 MΩ purity) was used to make  
210 solutions of each compound, for collecting blank filter samples in the aerosol generator and  
211 sampler system and to flush the system. Pure filtered air and chemical solutions were delivered to  
212 the atomizer to generate aerosol particles. Before collecting each compound, a 30-minute pre-flush  
213 with water was conducted to eliminate any residual material from the previous sample collection  
214 run. Subsequently, a water blank was collected onto the Teflon filter to identify any remaining  
215 contamination from prior samples. If contamination was identified, further cleaning was  
216 performed. Following this, each compound was collected on a Teflon filter using an IMPROVE  
217 aerosol sampler with sufficient mass to produce measurable water uptake in the sample above its  
218 deliquescence RH (Table 1). After completing these steps, the aerosol generator and sampler





219 underwent a 30-minute water flush to remove any deposited compounds, leaving it was  
220 contamination-free for subsequent runs. Pre-weights and post-weights of filters were recorded at  
221 least thrice on three separate days using a high-precision ultra-microbalance with a readability of  
222 0.1  $\mu\text{g}$  (model XP2U, Mettler–Toledo, USA) before and after sample collection. Following sample  
223 collection on the aerosol generator and sampler and prior to post-weighing, the collected samples  
224 were placed in a dry desiccator for a minimum of 24 hours to remove any residual water. The  
225 difference in the post-weight and pre-weight gives the amount of compound collected on the filter.  
226

227 **Table 1.** List of compounds collected using aerosol generator and sampler for water uptake  
228 measurements

Compound	Chemical Formula	Molecular Weight (g/mol)	Density (g/cc)	Deliquescence Relative Humidity (DRH) (%) <sup>a</sup>
Ammonium Sulfate	(NH <sub>4</sub> ) <sub>2</sub> (SO <sub>4</sub> )	132.14	1.77	78 – 82
Sodium Chloride	NaCl	58.44	2.16	73 – 77
D-Glucose	C <sub>6</sub> H <sub>12</sub> O <sub>6</sub>	180.156	1.56	90 <sup>b</sup>
Malonic Acid	C <sub>3</sub> H <sub>4</sub> O <sub>4</sub>	104.0615	1.619	65 – 76

<sup>a</sup>Peng et al., 2022; <sup>b</sup>Mochida & Kawamura (2004)

229

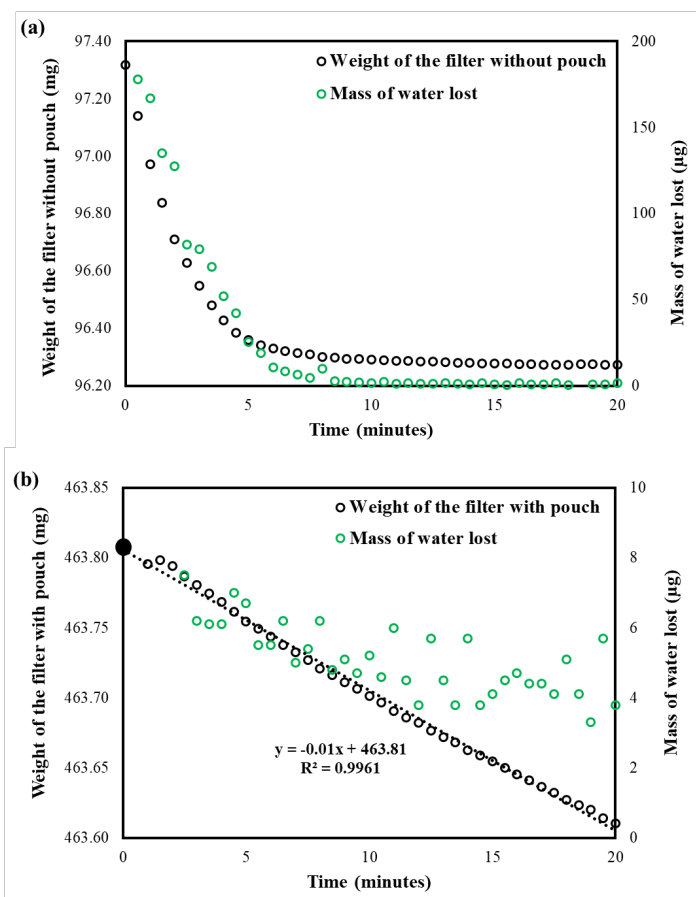
### 230 2.3. Water Uptake Measurements

231 After post-weighing, the dry particle-loaded filters (DS, post weighed filters with dry  
232 particles) were placed in sealed chambers at RHs of 84.3%, 90.8%, and 97.5%, and allowed to  
233 equilibrate for more than 24 hours. Subsequently, they were weighed to measure the water uptake  
234 by the solutes present on the filters. However, the weighing process did not proceed as expected;  
235 the filter weights were unstable on the balance, gradually decreasing until they reached their initial  
236 dry particle load weight (Fig. 2(a)). This indicated that the water taken up by compounds on the  
237 filter was evaporating during the weighing process, making it impossible to measure the water  
238 uptake at the chamber RH. Thus, there was a need for containment to prevent water loss during  
239 weighing.



240 **2.3.1. How can we minimize water loss?**

241 To limit water loss during the wet weighing of the filter, different types of pouches were  
 242 used to contain the filter and lock in the humidity, including plastic and antistatic zip lock bags.  
 243 However, these proved to be ineffective due to electrostatic interference during weighing and  
 244 hygroscopicity of the pouch material. Consequently, aluminum foil pouches were tested. Pouches  
 245 (approximately 5cm × 3cm × 1 cm) were fabricated from these foils, with three sides sealed. The  
 246 weights of these pouches were quite stable; therefore, they were tested further for possible use in  
 247 the water uptake measurements.



248

249 **Figure 2.** Weight of the filter and mass of water lost while weighing glucose from 97.5% RH:  
 250 (a) without a pouch and (b) with a pouch. The dashed line represents the linear extrapolation of  
 251 the observed filter weights to determine the actual wet filter weight (solid black circle) at the  
 252 time the sample was taken from the chamber.

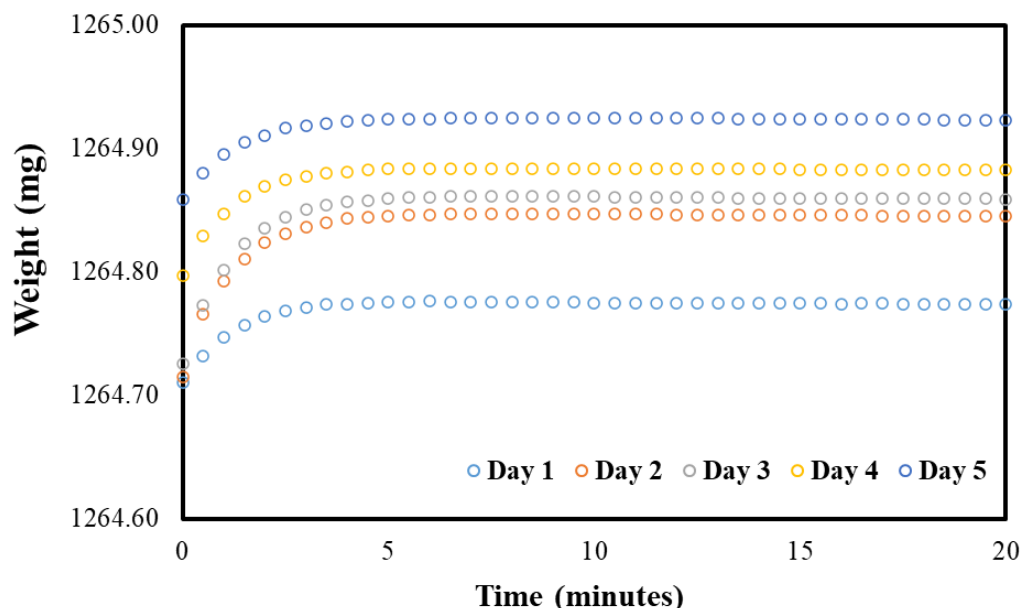


253 A dry particle-loaded filter was placed in a pouch and then placed in the chambers at the  
254 specified RH for more than 24 hours, with the fourth side open to allow water vapor in the air to  
255 interact with the particles on the filter. After equilibration and upon opening the chamber lid, the  
256 pouches were sealed immediately, and the time was recorded. Subsequently, the samples were  
257 transferred to the balance, and gravimetric readings were taken. The weight of the wet loaded  
258 sample (WSP, mass of the pouch with solute sample at measured RH) was recorded every 30  
259 seconds for 20 minutes (Fig 2b) to investigate how the wet weight of the filter with the pouch  
260 varied compared to that of the wet loaded filter without a pouch. The time taken for the sample  
261 transfer from the chamber to the first weight was also recorded.

262 Using a pouch to contain water loss while weighing proved to be effective. We observed a  
263 small, slow decrease that achieved steady-state (noisy due to being close to the uncertainty of the  
264 balance) after about 10 minutes in the wet weight of particulate filter with the pouch (fig 2(b)),  
265 compared to the large, rapid decrease without the pouch (fig. 2(a)). The initial increase in mass,  
266 followed by a linear decline required that the data be extrapolated from the linear region back to  
267 time zero to accurately determine the net water uptake by the solute on the filter (fig. 2(b), dotted  
268 line). These observations clearly suggest that the water loss from the filter can be nearly contained  
269 by using the pouch. Gold-coated aluminum foils were also tested and functioned similarly to  
270 regular aluminum foil (Fig. S2). Gold-coated foils were used in subsequent experiments because  
271 they come in separate sheets, making them easier to handle than rolled aluminum foil.

### 272 **2.3.2. Why does the pouch weight initially increase and then decrease?**

273 The initial weight gain of the pouch was perplexing, so we investigated by collecting wet  
274 weight of a pouch with a filter and pouch without a filter (Figure 3) every 30 seconds for over 20  
275 minutes. The same interval and duration of weighing were applied for all filters and tests unless  
276 stated otherwise. This procedure was repeated for five days. The weight increase in the initial  
277 minutes of weighing was calculated using the measured data shown in Figure 3 and compared it  
278 to the calculated change in air mass between wet and dry air using the psychrometric data to  
279 determine if dry air intrusion into the pouch was the cause of the weight gain.



280

281 **Figure 3.** Variation in the weight of the pouch with a Teflon filter over time starting when the  
 282 pouch is removed from the chamber (RH = 97.5%) and placed on the balance.

283 **2.3.2.1. Measurements**

284 The observed variation in the weight of the pouch (with a filter) over time during the  
 285 transition from measured RHs to the weighing balance, set at room RH, is depicted in Fig. 3.  
 286 Across all days and with or without a filter, the weight variation followed a similar pattern,  
 287 increasing for the first few minutes and then stabilizing.

288 The change in air mass for each day was determined by calculating the weight difference  
 289 between the initial time and the point at which the weighing reached a near-constant, as illustrated  
 290 in Eq. (6).

291 
$$m_i = m_z - m_0 \tag{6}$$

292 where,  $m_z$  is the weight of pouch at time ‘z’ where it becomes constant, and  $m_0$  is the weight of  
 293 pouch at zero time.

294 The average ( $\pm$ SD) increases in mass from zero time to the point where the pouch (with a  
 295 filter) weight became relatively constant for 84.3%, 90.8%, and 97.5% RHs was 95 ( $\pm$ 9)  $\mu$ g, 98  
 296 ( $\pm$ 56)  $\mu$ g, and 97 ( $\pm$ 34)  $\mu$ g, respectively.



### 297 2.3.2.2. Theoretical calculations using the Psychrometric Chart

298 The measured mass change was then compared to the calculated change in the mass of air  
299 from the chamber RHs to room RH from the specific volume (SV) using the psychrometric chart  
300 (PC) (source: [https://daytonashrae.org/psychrometrics/psychrometrics\\_si.html#start](https://daytonashrae.org/psychrometrics/psychrometrics_si.html#start)) at the known  
301 values of temperature and RHs. The assumption was made that the air inside the pouch was  
302 exchanged for room air within a few minutes. During this time, an increase in weight would be  
303 observed due to the displacement of less dense air (i.e. 97.5% RH) with denser air (~45% RH).  
304 The obtained SV from the PC was then inverted to determine the density ( $\rho$ ) of air at the respective  
305 RHs, as shown in Eq. (2) & (3),

$$306 \rho_r = \frac{1}{SV_r} \quad (2)$$

307

$$308 \rho_i = \frac{1}{SV_i} \quad (3)$$

309

310 where,  $\rho_i$  represents the air density at different RHs (i : 84.3%, 90.8%, and 97.5%), and  $SV_i$  is the  
311 specific volume at these RHs.  $\rho_r$  and  $SV_r$  represents the density and specific volume at room  
312 conditions (r).

313 The net change in air density ( $\Delta\rho$ ) from the measured relative humidities to room  
314 conditions is calculated using the Eq. (4),

$$315 \Delta\rho = \rho_r - \rho_i \quad (4)$$

316 The variation in the mass of air ( $m_i$ ) is calculated using the Eq. (5),

$$317 m_i = \Delta\rho \times V_p \quad (5)$$

318 where,  $m_i$  is the change in the mass of air from the measured RHs (84.3%, 90.8%, and 97.5%) to  
319 the room RH and  $V_p$  is the volume of the aluminum pouch.

320 The calculated air density and mass obtained at high and room RHs using PC are presented  
321 in Table S1. At higher RHs, the density of air in the pouch was lower, due to the increased  
322 concentration of water molecules at higher RHs, which have a lower molecular weight (18 g/mol)  
323 compared to that of air (29 g/mol). The calculated average net mass gain ( $\pm$ SD) from high RHs of



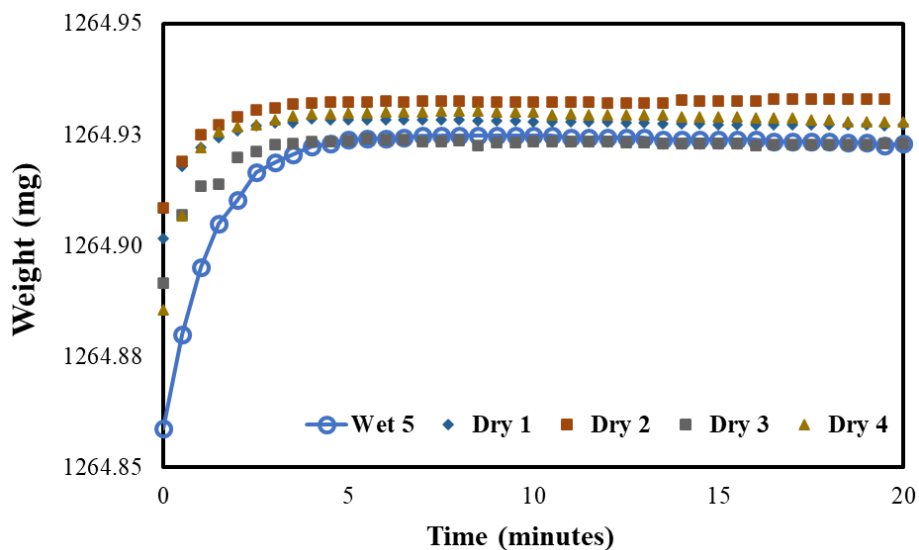
324 84.3%, 90.8%, and 97.5% to room RHs) was 197 ( $\pm 58$ )  $\mu\text{g}$ , 200 ( $\pm 52$ )  $\mu\text{g}$ , and 255 ( $\pm 54$ )  $\mu\text{g}$ ,  
325 respectively.

326 The theoretical increase in the mass of air was higher than the measured values. This is  
327 attributed to the air in the pouch being at a lower RH than the chamber RH at the initial weigh due  
328 to the time it takes to move the pouch from the glass chambers to the balance and an incomplete  
329 exchange of high RH to room RH air.

### 330 **2.3.3. Increasing weights of filter with pouch during repeated measurements over multiple** 331 **days**

332 While conducting water uptake measurements, we observed that the weight of the pouch  
333 with sampled filter was increasing from measurement to measurement even though the RH was  
334 not changing, leading to uncertainty in our water uptake measurements (Fig. 3). There was a  
335 consistent increase in the wet weight of the pouch with a filter for each consecutive day across all  
336 RHs (84.3%, 90.8%, and 97.5%), with average ( $\pm$ SD) increases of 13 ( $\pm 10$ )  $\mu\text{g}$ , 17 ( $\pm 9$ )  $\mu\text{g}$ , and  
337 37 ( $\pm 25$ )  $\mu\text{g}$ , respectively, as shown in Fig. 3 for 97.5% RH; results for 84.3% and 90.8% RH are  
338 shown in Figure S3. Similarly, for the pouch without a filter, there was increases in weight of 14  
339 ( $\pm 4$ )  $\mu\text{g}$ , 25 ( $\pm 11$ )  $\mu\text{g}$ , and 44 ( $\pm 7$ )  $\mu\text{g}$ , respectively (see Fig. S4).

340 To determine the cause of the mass increase, the following experiment was performed.  
341 After conducting water uptake measurements for five days, the pouches with blank filters were  
342 subsequently placed in a dry desiccator for a minimum of 24 hours and then weighed. This process  
343 was repeated for the next four days. The observed variations in the weights of the dried pouches  
344 are presented in Fig. 4 for 97.5% RH, and in Fig S3 for 84.3% and 90.8% RH. The weights of  
345 these pouches, measured across all RHs, remained fairly consistent, only varying by a few  
346 micrograms throughout the four days of measurement and did not exhibit a consistent trend in  
347 either increasing or decreasing weight. This suggests that after water adsorption onto the pouch,  
348 aluminum oxides are formed and remain stable at low RH. Considering these observations, it is  
349 prudent to account for water adsorption onto pouches when making water uptake measurements.

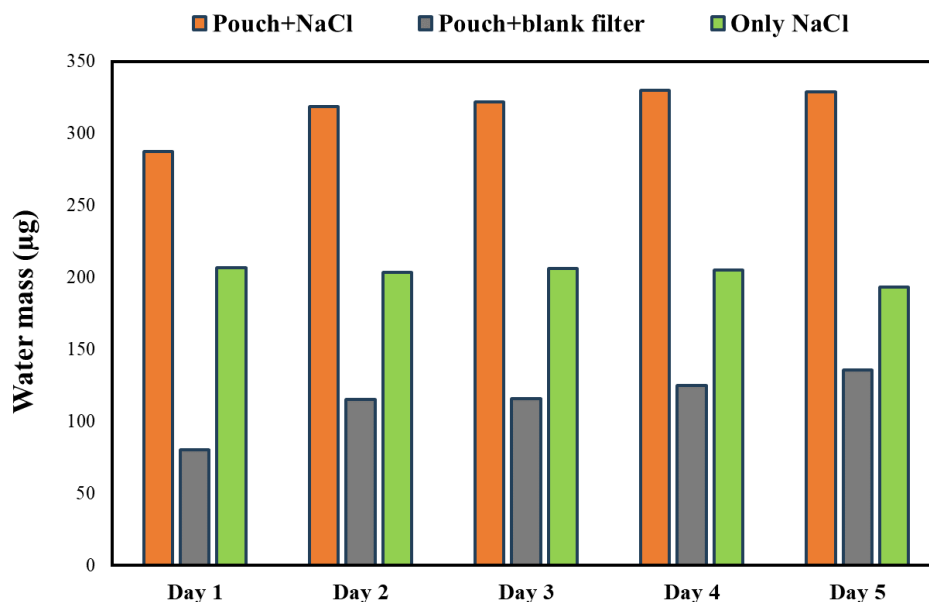


350

351 **Figure 4.** Variation in the dry weight of the pouch (with a filter) over time compared to the 5<sup>th</sup>  
 352 day wet measurement (97.5% RH)

353

354 By including a measurement blank, consisting of a pouch with a blank filter, alongside the  
 355 water uptake measurements using a pouch with a loaded filter, two issues are addressed: (i) water  
 356 absorption on the pouch itself and (ii) small day to day fluctuations in the balance due to changes  
 357 in meteorological and room conditions. The benefits of the measurement blank to account for water  
 358 absorption on the pouch are illustrated with a filter loaded with sodium chloride and exposed to  
 359 84.3% RH for five days. Figure 5 illustrates the water uptake of sodium chloride with the pouch,  
 360 the pouch with blank filter, and the net water uptake by sodium chloride, calculated as the  
 361 difference between the water uptake of the pouch with sodium chloride and the pouch with blank  
 362 filter. The water uptake of the pouch with sodium chloride filter increased day to day. However,  
 363 by subtracting the water uptake from the pouch with blank filter, the water uptake by sodium  
 364 chloride remained consistent day to day. Hence, to address pouch absorption, measurements were  
 365 conducted simultaneously on pouches with blank filters at the specified RHs and on pouches with  
 366 loaded filters; thus, for each compound, there were a total of six filters—three pouches with blanks,  
 367 one at 84.3%, 90.8%, and 97.5%, and similarly, three loaded filters in pouches at the same RH.



368

369

370 **Figure 5.** Water uptake by pouch with sodium chloride, pouch with blank filter, and only sodium  
371 chloride at 84.3% RH

372

### 373 2.4. Hygroscopic parameters estimation

374 Four parameters related to hygroscopicity are reported here: mass fraction of solute (mfs),  
375 molality, growth factor (GF). the water-to-solute ratio, which is the number of moles of water  
376 absorbed per mole of solute (compound). The calculations for these parameters are explained in  
377 the following sections.

#### 378 2.4.1. Mass fraction solute (mfs)

379 The solute mass fraction is the fraction of solute relative to the total mass of the solution.  
380 The mass of solution in the case of hygroscopic particles is the sum of solute's mass and the mass  
381 of water absorbed by the solute at a given RH, as illustrated in Eq. (7):

$$382 \text{ mfs} = \frac{\text{mass of solute } (\mu\text{g})}{\text{mass of solute } (\mu\text{g}) + \text{mass of water uptaken by the solute } (\mu\text{g})} \quad (7)$$

383

384





### 385 2.4.2. Molality (m)

386 Molality is the moles of solute dissolved in a certain mass of water, as illustrated in Eq.  
387 (8):

$$388 \text{ Molality (m, mol/kg)} = \frac{\text{no. of moles of solute}}{\text{mass of solvent (water absorbd by the solute)}} \quad (8)$$

### 389 2.4.3. Growth Factor

390 The growth factor (GF) of the dry particles at the measured RHs is estimated from the ratio  
391 of wet particle diameter to the dry particle diameter, as shown in Eq. (9):

$$392 \text{ GF}_j = \frac{D_{w,j}}{D_{dry}} \quad (9)$$

393 where,  $D_{w,j}$  is the diameter of the wet particle at RH,  $j$  and  $D_{dry}$  is the diameter of dry particle. The  
394 detailed calculations of GF at the respective RH are explained in Eq. (10) to Eq. (14):

$$395 \text{ Volume of the dry solute, } V_{dry} = \frac{\text{mass of solute}}{\text{density of solute}} \quad (10)$$

$$396 \text{ Volume of adsorbed water onto the solute, } V_{water} = \frac{\text{mass of water}}{\text{density of water}} \quad (11)$$

$$397 \text{ Total volume of the wet particle, } V_{wet} = V_{dry} + V_{water} \quad (12)$$

$$398 \text{ Average diameter of the wet particle, } D_{wet} = 2 \times \left( \frac{3V_{wet}}{4\pi} \right)^{\frac{1}{3}} \quad (13)$$

$$399 \text{ Average diameter of the dry particle, } D_{dry} = 2 \times \left( \frac{3V_{dry}}{4\pi} \right)^{\frac{1}{3}} \quad (14)$$

### 400 2.4.4. Water-to-solute ratio

401 Equation 15 gives the water/solute (W/S) of the sample on the filter in terms of the  
402 measured quantities:

$$403 \frac{\text{Water}}{\text{Solute}} = \frac{(\text{wet sample with pouch} - \text{dry sample with pouch}) - (\text{wet blank with pouch} - \text{dry blank with pouch})}{\text{dry sample} - \text{dry blank}} \times \frac{MW_s}{MW_w} \quad (15)$$

405 where, wet sample with pouch (WSP) is the mass of the pouch and sampled filter at high RH, dry  
406 sample with pouch (DSP) is the mass of the pouch with particles on the filter at dry conditions,



407 wet blank with pouch (WBP) is the mass of the pouch with blank filter at high RH, dry blank with  
408 pouch (DBP) is the mass of the pouch with blank filter at dry conditions, dry sample (DS) is the  
409 mass of the filter with particles on the filter at dry condition, and dry blank (DB) is the mass of the  
410 blank filter.  $MW_s$  and  $MW_w$  are the molecular weight of solute and water, respectively. All are in  
411 the units of milligrams (mg), except MW, mol/gm.

## 412 2.5. Uncertainty in the measured water-to-solute (W/S) ratio

413 The uncertainty of the measured water-to-solute ratio was determined using the partial  
414 derivatives of the input parameters employed in calculating the W/S ratio.

415 From Eq. (15), the W/S ratio can be written as

$$416 \quad \frac{W}{S} = \frac{(WSP-DS)-(WBP-DBP)}{DS-DB} \times \frac{MW_s}{MW_w} \quad (16)$$

417 The sensitivity of the W/S ratio to the input variables ( $X$ ) were calculated using partial derivatives  
418  $(\frac{\partial(W/S)}{\partial(X)})$ , as illustrated in Eq. (17) through (22):

$$419 \quad \left| \frac{\partial(W/S)}{\partial(WSP)} \right| = \left| \frac{1}{DS-DB} \right| \quad (17)$$

$$420 \quad \left| \frac{\partial(W/S)}{\partial(DSP)} \right| = \left| \frac{1}{DB-DS} \right| \quad (18)$$

$$421 \quad \left| \frac{\partial(W/S)}{\partial(WBP)} \right| = \left| \frac{1}{DB-DS} \right| \quad (19)$$

$$422 \quad \left| \frac{\partial(W/S)}{\partial(DBP)} \right| = \left| \frac{1}{DS-DB} \right| \quad (20)$$

$$423 \quad \left| \frac{\partial(W/S)}{\partial(DS)} \right| = \left| \frac{-(WSP-DS)+(WBP-DBP)}{(DS-DB)^2} \right| \quad (21)$$

$$424 \quad \left| \frac{\partial(W/S)}{\partial(DB)} \right| = \left| \frac{(WSP-DS)-(WBP-DBP)}{(DS-DB)^2} \right| \quad (22)$$

425 The uncertainty contribution  $\delta X$  of each input variable ( $X$ ) to the measured W/S ratio was  
426 estimated using Eq. (23):

$$427 \quad \delta X = \left| \frac{\partial(W/S)}{\partial X} \right| \times \sigma(X) \quad (23)$$

428 where,  $\sigma(X)$  is the standard deviation of each input parameter ( $X$ ).



429 The overall uncertainty in the measured W/S was calculated using Eq. (24):

$$430 \quad \delta(W/S) = \sum \left( \left| \frac{\partial(W/S)}{\partial(X)} \right| \times \sigma(X) \right) \quad (24)$$

431 The percentage uncertainty contribution by each input variable to total uncertainty in the W/S ratio  
432 was calculated using Eq. (25):

$$433 \quad \frac{\delta(X)}{W/S} \times 100 \quad (25)$$

### 434 **3. Results and Discussion**

#### 435 **3.1. Derived hygroscopic parameters**

436 Table 2 shows the hygroscopic parameters derived from the measurements, including  
437 water-to-solute (W/S) ratio, mfs, molality, and GF at the measured RHs for ammonium sulfate,  
438 sodium chloride, glucose, and malonic acid. The observed water uptake increased from 84.3% to  
439 97.5% RH for all compounds. For example, the observed W/S ratio of sodium chloride i.e. moles  
440 of water absorbed per mole of sodium chloride was 14.62 at 84.3% RH, 19.8 at 90.8% RH and 86  
441 at 97.5% RH. Similarly, for ammonium sulfate, glucose, and malonic acid, the W/S increased from  
442 an RH of 84.3% to 97.5% by factors of 5.0, 4.8, and 6.9, respectively. Conversely, the mfs and  
443 molality decreased with increasing RH for all the measured compounds. For example, the mfs of  
444 malonic acid was 0.47 at 84.3% RH, but only 0.11 at 97.5% RH. Similarly, the observed molality  
445 for malonic acid was 8.63 at 84.3% RH, which reduced to 1.25 at 97.5% RH.

446

447

448

449

450

451

452

453



454 **Table 2.** Derived hygroscopic parameters from this study’s developed methodology (n = 5)

	RH=84.3%		RH=90.8%		RH=97.5%	
	Mean	SD	Mean	SD	Mean	SD
<b>Ammonium sulfate</b>						
<b>W/S</b>	9.26	0.71	16.9	1.24	45.69	0.43
<b>MFS</b>	0.44	0.02	0.3	0.02	0.14	0.00
<b>Molality</b>	6.03	0.48	3.3	0.26	1.22	0.01
<b>GF</b>	1.47	0.03	1.7	0.04	2.29	0.01
<b>Sodium chloride</b>						
<b>W/S</b>	14.62	0.40	19.80	0.32	85.98	2.53
<b>MFS</b>	0.18	0	0.14	0	0.04	0
<b>Molality</b>	3.80	0.11	2.80	0.05	0.65	0.02
<b>GF</b>	2.23	0.003	2.45	0.02	3.88	0.04
<b>Glucose</b>						
<b>W/S</b>	6.82	0.17	9.62	0.94	33.09	1.40
<b>MFS</b>	0.59	0.01	0.51	0.02	0.23	0.01
<b>Molality</b>	8.14	0.21	5.81	0.57	1.68	0.07
<b>GF</b>	1.29	0.01	1.36	0.03	1.83	0.02
<b>Malonic acid</b>						
<b>W/S</b>	6.45	0.27	10.93	0.55	44.69	3.39
<b>MFS</b>	0.47	0.01	0.35	0.01	0.11	0.01
<b>Molality</b>	8.63	0.35	5.09	0.26	1.25	0.09
<b>GF</b>	1.27	0.01	1.6	0.02	2.38	0.05

455

456 In this study, the water uptake measurements for each compound at each specific RH were  
 457 repeated over five different days to investigate the repeatability of the determined hygroscopic  
 458 parameters. The variability (standard deviation) in the observed hygroscopic parameters, as shown  
 459 in Table 2, is small. For instance, the relative standard deviation (RSD,  $SD \div \text{mean}$ ) of the growth  
 460 factor for malonic acid at all RHs was less than 0.5%. This observation clearly indicates that the  
 461 variability of measured hygroscopic parameters at the same RH for each compound between  
 462 different experiment days is minimal, highlighting the repeatability of this methodology. In  
 463 addition, to examine the reproducibility of this methodology, we repeated the water uptake  
 464 measurement for the malonic acid compound at 97.5% RH with different masses (48.8µg and  
 465 130.4 µg) and estimated the hygroscopic parameters. We observed insignificant differences  
 466 (~0.4%) in the water uptake parameters of malonic acid at 97.5% RH between the two experiments.  
 467 These observations indicate that the developed methodology can reproducibly assess the  
 468 hygroscopicity of particles collected on Teflon filters.



469 In our study, we recorded the wet weight every 30 seconds over 20 minutes to estimate the  
470 hygroscopic parameters. However, we evaluated if this length of time was necessary by calculating  
471 the GFs for each compound at the measured RHs for 5, 10, and 15-minute intervals and compared  
472 them with the GFs using the 20-minutes interval, shown in Figure S5. There was no significant  
473 difference between the GFs estimated using the 5, 10, 15 and 20-minute intervals. For future  
474 studies, it is unnecessary to take wet weighing for 20 minutes; and taking wet weights every 30  
475 seconds over a 5-minute period is sufficient to determine hygroscopic parameters.

### 476 **3.2. Comparison of estimated hygroscopic parameters with previous studies**

477 Most of the prior studies reported the water uptake in terms of GFs with few reported in terms of  
478 mfs and molality so we will focus our comparisons on GF measurements. The estimated average  
479 GFs for each compound at the measured RHs were compared with previous studies, depicted in  
480 Fig. 6. These studies used techniques such as HTDMA and EDB to derive GF. These studies  
481 typically examined RH levels of 90% or lower, except for Mikhailov et al., (2024), who estimated  
482 GFs for ammonium sulfate and glucose at RH levels up to 99.9%. Additionally, the estimated GFs  
483 for compounds were compared with values provided by the thermodynamic model, E-AIM  
484 (<http://www.aim.env.uea.ac.uk/aim/aim.php>), which has been widely used to assess the water  
485 uptake of inorganic compounds for over three decades. The estimated GF for sodium chloride of  
486 2.23 at 84.3% RH was similar to values reported in previous studies (M. Cheng & Kuwata, 2023;  
487 Hu et al., 2010; Peng et al., 2016), which ranged from 2–2.22. Similarly, at 90.8% RH, the  
488 observed GF for sodium chloride of 2.45 was close to previous findings (M. Cheng & Kuwata,  
489 2023; Peng et al., 2016; Zieger et al., 2017), which ranged from 2.20–2.40. For ammonium sulfate,  
490 the observed GFs at 84.3%, 90.8, and 97.5% RH were 1.47, 1.7, 2.29, respectively, which are  
491 similar to those of previous studies (Bouzidi et al., 2020; M. Cheng & Kuwata, 2023; Choi &  
492 Chan, 2002; Cruz & Pandis, 2000; Denjean et al., 2014; Hämeri et al., 2002; Hu et al., 2010;  
493 Koehler et al., 2006; Liu et al., 2016; Mikhailov et al., 2024; Prenni et al., 2001; Sjogren et al.,  
494 2007), which were 1.49–1.60, 1.70–1.79, and 2.3, respectively. Likewise, for glucose, at 84.3%,  
495 90.8%, and 97.5% RH, the observed GFs fell within the ranges reported in earlier studies (Lei et  
496 al., 2023; Mikhailov et al., 2024; Mochida & Kawamura, 2004), which were 1.2–1.5, 1.3–1.65,  
497 and 1.8 respectively. For malonic acid, the observed GFs at 84.3% and 90.8% RH were consistent  
498 with the ranges found in previous studies (Bouzidi et al., 2020; Peng et al., 2001; Pope et al., 2010;



499 Prenni et al., 2001). The measured GF for ammonium sulfate and sodium chloride at all RH levels  
500 agreed well with the E-AIM model values, except at 97.5% RH. The observed GF for ammonium  
501 sulfate at 97.5% in this study was slightly lower than the value reported by E-AIM, differing by a  
502 factor of 1.11. For sodium chloride, it was higher by a factor of 1.12. Changes in water uptake near  
503 saturation RH are steep, and even slight variations in RH can significantly affect the GF. This  
504 likely explains the slight differences between this study and the E-AIM at 97.5% RH.

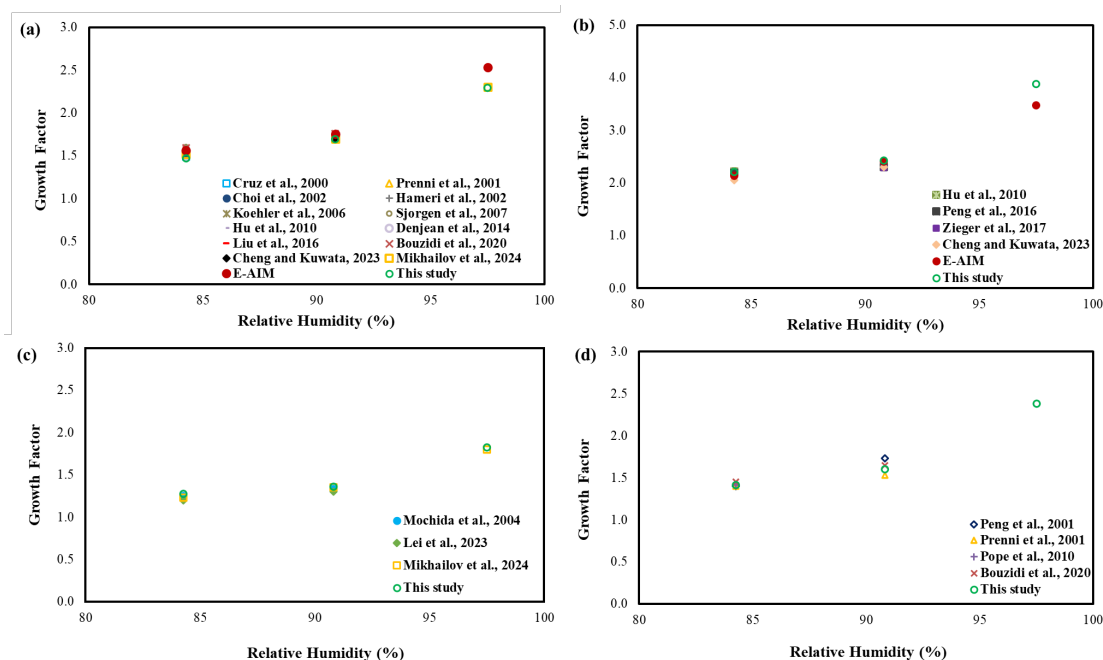
505 This study's observed average mfs of malonic acid for 84.3%, 90.8%, and 97.5% RH was  
506 0.47, 0.35, and 0.11, respectively, which are similar to those of previous studies (0.475, 0.37–0.38,  
507 and 0.11, respectively) as reported by Koehler et al. (2006) and Maffia & Meirelles (2001). In the  
508 same way, for other compounds, the observed mfs are closely matched with those of previous  
509 studies (ammonium sulfate: 0.37–0.42, 0.3–0.32, and 0.1–0.12 (Chan et al., 1992; Kim et al., 1994;  
510 Kreidenweis et al., 2005; Mikhailov et al., 2024); glucose: 0.60, 0.44–0.46, 0.25 (Mikhailov et al.,  
511 2024; Peng et al., 2001); sodium chloride: 0.175, 0.04 (Kreidenweis et al., 2005)). Few studies  
512 have reported water uptake in terms of molality, and the observed molality for all the compounds  
513 in this study were close to the range of those reported in previous studies (Ammonium sulfate: ~4–  
514 6.5, 3–3.2, and 1 (Y. Cheng et al., 2015; Mikhailov et al., 2024; Zamora & Jacobson, 2013),  
515 Glucose: ~5.25–8, 4.7, and 1 (Lei et al., 2023; Mikhailov et al., 2024; Zamora et al., 2011), Malonic  
516 acid: ~8.5, 5.7, and 1.25 (Lee & Hildemann, 2013)), and sodium chloride: ~4.25, 2.2, and 0.75  
517 (Zamora & Jacobson, 2013)).

518

519

520

521



522

523 **Figure 6.** Comparison of estimated growth factor for (a) Ammonium sulfate, (b) sodium  
524 chloride, (c) Glucose, and (d) Malonic acid with previous studies

525

526 The above comparisons validates the accuracy and reliability of the methodology used in  
527 this study. Therefore, the water uptake of particles collected on Teflon filters can be effectively  
528 assessed using the developed methodology.

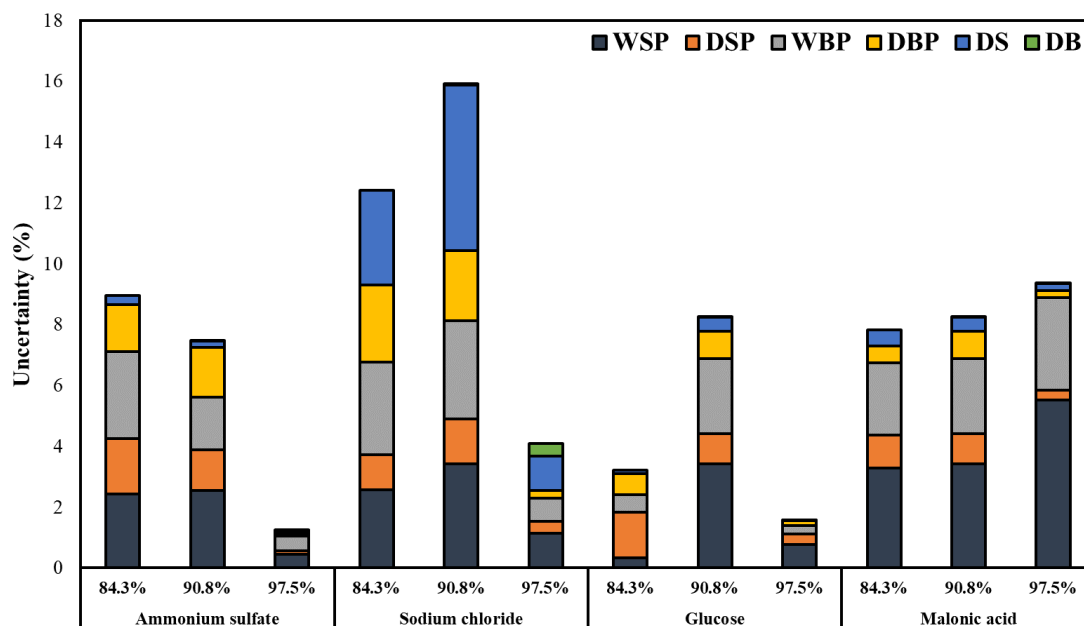
### 529 3.3. Estimated uncertainties in the W/S ratio

530 The estimated uncertainties in the W/S ratio using this study’s methodology are depicted  
531 in Fig. 7. Overall, the uncertainty for almost all the measured compounds at measured RHs was  
532 below 10%, except for sodium chloride at 84.3% and 90.8%, which had uncertainties of 12% and  
533 15%, respectively. WSP and WBP contributed the most to the overall W/S uncertainty, followed  
534 by DSP and DBP, with DS and DB contributing the least for all the measured compounds, except  
535 sodium chloride. For sodium chloride, consistent water uptake was observed across all five  
536 measured days, as exemplified by the net water uptake at 84% RH, shown in Fig. 5. However, for  
537 sodium chloride, the major uncertainty was associated with DS, unlike other compounds. A  
538 plausible reason for this discrepancy is the smaller mass of sodium chloride (45, 39.5, and 27.8 $\mu$ g



539 for 84.3, 90.8, and 97.5% RHs, respectively) compared to other compounds which averaged 122,  
 540 274 and 88  $\mu\text{g}$  for ammonium sulfate, glucose, and malonic acid, respectively for all three RHs  
 541 The lower mass increases uncertainty due to the limitations in the precision of the balance.. For  
 542 sodium chloride at 97.5%, water uptake was more than 3 times higher than at 84.3 and 90.8% RH  
 543 resulting in lower uncertainty at 97.5%. This discrepancy is inherent in the W/S ratio calculation,  
 544 as the mass of solute is in the denominator. Nevertheless, it is important to note that this uncertainty  
 545 is not inherent in the developed methodology but rather caused by the lower mass used for sodium  
 546 chloride in the water uptake measurements. To reduce this uncertainty, based on our observations,  
 547 we recommend using a larger mass: at least  $50\mu\text{g}$  for hygroscopic compounds like sodium chloride,  
 548  $100\mu\text{g}$  for medium hygroscopic compounds like glucose, and more than  $200\mu\text{g}$  for less  
 549 hygroscopic compounds.

550



551

552 **Figure 7.** Estimated uncertainties in the measured water-to-solute ratio at different RHs.

553

554

555





556 **4. Conclusion**

557 In this study, we developed a novel methodology to assess the water uptake of particulate  
558 samples collected on Teflon filters. By using filter samples, the chemical composition of ambient  
559 or chamber samples can be measured as well as water uptake, something neither HTDMA nor  
560 EDB can do for complex mixtures. The advantage of this method is that it enables hygroscopicity  
561 to be related to chemical composition. Additionally, this method can be used to measure water uptake  
562 above 90% RH, which is typically not done with HTDMA measurements.

563 Constant humidity solutions were employed to maintain specific RH and enable measurements as  
564 high as ~97%. Hygroscopic parameters, including the W/S ratio, GF, molality, and the mfs, were  
565 estimated from water uptake measurements for ammonium sulfate, sodium chloride, glucose, and  
566 malonic acid at RH levels of 84.3%, 90.8%, and 97.5%. As expected, the water uptake increased  
567 with higher RH for all compounds. The observed GFs in this study were consistent with those  
568 reported in previous studies for all the measured compounds at the examined RH levels, and similar  
569 to modelled values for the inorganics highlighting the accuracy of this method. The overall  
570 uncertainty in the observed W/S ratio was less than 10% for most of the compound/RH  
571 combinations measured, further highlighting robustness and precision of this new method.

572 **Author Contributions**

573 ASW and AMD conceived of the project. NR developed the water uptake methodology, performed  
574 the laboratory work and data analysis, created the figures and tables, and wrote and edited the  
575 manuscript. ASW and AMD provided leadership for the project, including mentoring and  
576 supervising NR in the laboratory work, methodology development and data analysis, and reviewed  
577 and edited the manuscript.

578 **Competing interests**

579 The contact author has declared that none of the authors has any competing interests.

580 **Acknowledgements**

581 We would like to thank the Department of Energy (DOE), USA, for funding this project (grant no.  
582 DE-SC0023087). We also acknowledge the support of undergraduate students Lucas Wang and  
583 Alexander Velasco in the laboratory measurements.



584 **References**

- 585 Boreddy, S. K. R., Kawamura, K., & Jung, J. (2014). Hygroscopic properties of particles nebulized  
586 from water extracts of aerosols collected at Chichijima Island in the western North Pacific:  
587 An outflow region of Asian dust. *Journal of Geophysical Research: Atmospheres*, *119*(1),  
588 167–178. <https://doi.org/10.1002/2013JD020626>
- 589 Boris, A. J., Takahama, S., Weakley, A. T., Debus, B. M., Fredrickson, C. D., Esparza-Sanchez,  
590 M., Burki, C., Reggente, M., Shaw, S. L., Edgerton, E. S., & Dillner, A. M. (2019).  
591 Quantifying organic matter and functional groups in particulate matter filter samples from  
592 the southeastern United States – Part 1: Methods. *Atmospheric Measurement Techniques*,  
593 *12*(10), 5391–5415. <https://doi.org/10.5194/amt-12-5391-2019>
- 594 Bouzidi, H., Zuend, A., Ondráček, J., Schwarz, J., & Ždímal, V. (2020). Hygroscopic behavior of  
595 inorganic–organic aerosol systems including ammonium sulfate, dicarboxylic acids, and  
596 oligomer. *Atmospheric Environment*, *229*, 117481.  
597 <https://doi.org/10.1016/j.atmosenv.2020.117481>
- 598 Chan, C. K., Flagan, R. C., & Seinfeld, J. H. (1992). Water activities of  $\text{NH}_4\text{NO}_3/(\text{NH}_4)_2\text{SO}_4$   
599 solutions. *Atmospheric Environment. Part A. General Topics*, *26*(9), 1661–1673.  
600 [https://doi.org/10.1016/0960-1686\(92\)90065-S](https://doi.org/10.1016/0960-1686(92)90065-S)
- 601 Chan, C. K., Ha, Z., & Choi, M. Y. (2000). Study of water activities of aerosols of mixtures of  
602 sodium and magnesium salts. *Atmospheric Environment*, *34*(28), 4795–4803.  
603 [https://doi.org/10.1016/S1352-2310\(00\)00252-1](https://doi.org/10.1016/S1352-2310(00)00252-1)
- 604 Cheng, M., & Kuwata, M. (2023). Development of the low-temperature hygroscopicity tandem  
605 differential mobility analyzer (Low-T HTDMA) and its application to  $(\text{NH}_4)_2\text{SO}_4$  and  
606 NaCl particles. *Journal of Aerosol Science*, *168*, 106111.  
607 <https://doi.org/10.1016/j.jaerosci.2022.106111>
- 608 Cheng, Y., Su, H., Koop, T., Mikhailov, E., & Pöschl, U. (2015). Size dependence of phase  
609 transitions in aerosol nanoparticles. *Nature Communications*, *6*(1), 5923.  
610 <https://doi.org/10.1038/ncomms6923>
- 611 Choi, M. Y., & Chan, C. K. (2002). The Effects of Organic Species on the Hygroscopic Behaviors  
612 of Inorganic Aerosols. *Environmental Science & Technology*, *36*(11), 2422–2428.  
613 <https://doi.org/10.1021/es0113293>



- 614 Clegg, S. L., Brimblecombe, P., & Wexler, A. S. (1998). Thermodynamic Model of the System H  
615  $^+ -\text{NH}_4^+ -\text{SO}_4^{2-} -\text{NO}_3^- -\text{H}_2\text{O}$  at Tropospheric Temperatures. *The Journal of Physical*  
616 *Chemistry A*, 102(12), 2137–2154. <https://doi.org/10.1021/jp973042r>
- 617 Cohen, M. D., Flagan, R. C., & Seinfeld, J. H. (1987). Studies of concentrated electrolyte solutions  
618 using the electrodynamic balance. 1. Water activities for single-electrolyte solutions. *The*  
619 *Journal of Physical Chemistry*, 91(17), 4563–4574. <https://doi.org/10.1021/j100301a029>
- 620 Cruz, C. N., & Pandis, S. N. (2000). Deliquescence and Hygroscopic Growth of Mixed  
621 Inorganic–Organic Atmospheric Aerosol. *Environmental Science & Technology*, 34(20),  
622 4313–4319. <https://doi.org/10.1021/es9907109>
- 623 Denjean, C., Formenti, P., Picquet-Varrault, B., Katrib, Y., Pangui, E., Zapf, P., & Doussin, J. F.  
624 (2014). A new experimental approach to study the hygroscopic and optical properties of  
625 aerosols: Application to ammonium sulfate particles. *Atmospheric Measurement*  
626 *Techniques*, 7(1), 183–197. <https://doi.org/10.5194/amt-7-183-2014>
- 627 Fredenslund, A., Jones, R. L., & Prausnitz, J. M. (1975). Group-contribution estimation of activity  
628 coefficients in nonideal liquid mixtures. *AIChE Journal*, 21(6), 1086–1099.  
629 <https://doi.org/10.1002/aic.690210607>
- 630 Greenspan, L. (1976). Humidity Fixed Points of Binary Saturated Aqueous Solutions. *Journal of*  
631 *Research of the National Bureau of Standards - A. Physics and Chemistry*, 81A, 1.
- 632 Gupta, T., Rajeev, P., & Rajput, R. (2022). Emerging Major Role of Organic Aerosols in  
633 Explaining the Occurrence, Frequency, and Magnitude of Haze and Fog Episodes during  
634 Wintertime in the Indo Gangetic Plain. *ACS Omega*, 7(2), 1575–1584.  
635 <https://doi.org/10.1021/acsomega.1c05467>
- 636 Hämeri, K., Charlson, R., & Hansson, H. (2002). Hygroscopic properties of mixed ammonium  
637 sulfate and carboxylic acids particles. *AIChE Journal*, 48(6), 1309–1316.  
638 <https://doi.org/10.1002/aic.690480617>
- 639 Han, S., Hong, J., Luo, Q., Xu, H., Tan, H., Wang, Q., Tao, J., Zhou, Y., Peng, L., He, Y., Shi, J.,  
640 Ma, N., Cheng, Y., & Su, H. (2022). Hygroscopicity of organic compounds as a function  
641 of organic functionality, water solubility, molecular weight, and oxidation level.  
642 *Atmospheric Chemistry and Physics*, 22(6), 3985–4004. [https://doi.org/10.5194/acp-22-](https://doi.org/10.5194/acp-22-3985-2022)  
643 3985-2022



- 644 Haseeb, M., Tahir, Z., Mahmood, S. A., Batool, S., Tariq, A., Lu, L., & Soufan, W. (2024). Spatio-  
645 temporal assessment of aerosol and cloud properties using MODIS satellite data and a  
646 HYSPLIT model: Implications for climate and agricultural systems. *Atmospheric*  
647 *Environment: X*, 21, 100242. <https://doi.org/10.1016/j.aeaoa.2024.100242>
- 648 Hu, D., Qiao, L., Chen, J., Ye, X., Yang, X., Cheng, T., & Fang, W. (2010). Hygroscopicity of  
649 Inorganic Aerosols: Size and Relative Humidity Effects on the Growth Factor. *Aerosol and*  
650 *Air Quality Research*, 10(3), 255–264. <https://doi.org/10.4209/aaqr.2009.12.0076>
- 651 Jathar, S. H., Mahmud, A., Barsanti, K. C., Asher, W. E., Pankow, J. F., & Kleeman, M. J. (2016).  
652 Water uptake by organic aerosol and its influence on gas/particle partitioning of secondary  
653 organic aerosol in the United States. *Atmospheric Environment*, 129, 142–154.  
654 <https://doi.org/10.1016/j.atmosenv.2016.01.001>
- 655 Kohli, R.K., Davis, R. D., & Davies, J. F. (2023). Tutorial: Electrodynamic balance methods for  
656 single particle levitation and the physicochemical analysis of aerosol. *Journal of Aerosol*  
657 *Science*, 174, 106255. <https://doi.org/10.1016/j.jaerosci.2023.106255>
- 658 Kim, Y. P., Pun, B. K.-L., Chan, C. K., Flagan, R. C., & Seinfeld, J. H. (1994). Determination of  
659 Water Activity in Ammonium Sulfate and Sulfuric Acid Mixtures Using Levitated Single  
660 Particles. *Aerosol Science and Technology*, 20(3), 275–284.  
661 <https://doi.org/10.1080/02786829408959683>
- 662 Kim, Y. P., & Seinfeld, J. H. (1995). Atmospheric Gas–Aerosol Equilibrium: III. Thermodynamics  
663 of Crustal Elements  $\text{Ca}^{2+}$ ,  $\text{K}^{+}$ , and  $\text{Mg}^{2+}$ . *Aerosol Science and Technology*, 22(1), 93–  
664 110. <https://doi.org/10.1080/02786829408959730>
- 665 Koehler, K. A., Kreidenweis, S. M., DeMott, P. J., Prenni, A. J., Carrico, C. M., Ervens, B., &  
666 Feingold, G. (2006). Water activity and activation diameters from hygroscopicity data –  
667 Part II: Application to organic species. *Atmos. Chem. Phys.*
- 668 Kreidenweis, S. M., Koehler, K., DeMott, P. J., Prenni, A. J., Carrico, C., & Ervens, B. (2005).  
669 Water activity and activation diameters from hygroscopicity data – Part I: Theory and  
670 application to inorganic salts. *Atmos. Chem. Phys.*
- 671 Krumgalz, B.S. (2018). Temperature Dependence of Mineral Solubility in Water. Part 3.  
672 Alkaline and Alkaline Earth Sulfates. *Journal of Physical and Chemical Reference Data*,  
673 47, 023101.



- 674 Laskina, O., Morris, H. S., Grandquist, J. R., Qin, Z., Stone, E. A., Tivanski, A. V., & Grassian,  
675 V. H. (2015). Size Matters in the Water Uptake and Hygroscopic Growth of  
676 Atmospherically Relevant Multicomponent Aerosol Particles. *The Journal of Physical  
677 Chemistry A*, 119(19), 4489–4497. <https://doi.org/10.1021/jp510268p>
- 678 Lee, A. K. Y., Ling, T. Y., & Chan, C. K. (2008). Understanding hygroscopic growth and phase  
679 transformation of aerosols using single particle Raman spectroscopy in an electrodynamic  
680 balance. *Faraday Discuss.*, 137, 245–263. <https://doi.org/10.1039/B704580H>
- 681 Lee, J. Y., & Hildemann, L. M. (2013). Comparisons between Hygroscopic Measurements and  
682 UNIFAC Model Predictions for Dicarboxylic Organic Aerosol Mixtures. *Advances in  
683 Meteorology*, 2013, 1–9. <https://doi.org/10.1155/2013/897170>
- 684 Lei, T., Su, H., Ma, N., Pöschl, U., Wiedensohler, A., & Cheng, Y. (2023). Size-dependent  
685 hygroscopicity of levoglucosan and D-glucose aerosol nanoparticles. *Atmospheric  
686 Chemistry and Physics*, 23(8), 4763–4774. <https://doi.org/10.5194/acp-23-4763-2023>
- 687 Li, J., Carlson, B. E., Yung, Y. L., Lv, D., Hansen, J., Penner, J. E., Liao, H., Ramaswamy, V.,  
688 Kahn, R. A., Zhang, P., Dubovik, O., Ding, A., Lacis, A. A., Zhang, L., & Dong, Y. (2022).  
689 Scattering and absorbing aerosols in the climate system. *Nature Reviews Earth &  
690 Environment*, 3(6), 363–379. <https://doi.org/10.1038/s43017-022-00296-7>
- 691 Lide, D. R. CRC Handbook of Chemistry and Physics; CRC press, 2004; Vol. 85.
- 692 Liu, Q., Jing, B., Peng, C., Tong, S., Wang, W., & Ge, M. (2016). Hygroscopicity of internally  
693 mixed multi-component aerosol particles of atmospheric relevance. *Atmospheric  
694 Environment*, 125, 69–77. <https://doi.org/10.1016/j.atmosenv.2015.11.003>
- 695 Luo, Q., Hong, J., Xu, H., Han, S., Tan, H., Wang, Q., Tao, J., Ma, N., Cheng, Y., & Su, H. (2020).  
696 Hygroscopicity of amino acids and their effect on the water uptake of ammonium sulfate  
697 in the mixed aerosol particles. *Science of The Total Environment*, 734, 139318.  
698 <https://doi.org/10.1016/j.scitotenv.2020.139318>
- 699 Maffia, M. C., & Meirelles, A. J. A. (2001). Water Activity and pH in Aqueous Polycarboxylic  
700 Acid Systems. *Journal of Chemical & Engineering Data*, 46(3), 582–587.  
701 <https://doi.org/10.1021/je0002890>
- 702 Marsh, A., Rovelli, G., Miles, R. E. H., & Reid, J. P. (2019). Complexity of Measuring and  
703 Representing the Hygroscopicity of Mixed Component Aerosol. *The Journal of Physical  
704 Chemistry A*, 123(8), 1648–1660. <https://doi.org/10.1021/acs.jpca.8b11623>



- 705 Mikhailov, E. F., Pöhlker, M. L., Reinmuth-Selzle, K., Vlasenko, S. S., Krüger, O. O., Fröhlich-  
706 Nowoisky, J., Pöhlker, C., Ivanova, O. A., Kiselev, A. A., Kremper, L. A., & Pöschl, U.  
707 (2021). Water uptake of subpollen aerosol particles: Hygroscopic growth, cloud  
708 condensation nuclei activation, and liquid–liquid phase separation. *Atmospheric Chemistry  
709 and Physics*, 21(9), 6999–7022. <https://doi.org/10.5194/acp-21-6999-2021>
- 710 Mikhailov, E. F., Vlasenko, S. S., & Kiselev, A. A. (2024). Water activity and surface tension of  
711 aqueous ammonium sulfate and D-glucose aerosol nanoparticles. *Atmospheric Chemistry  
712 and Physics*, 24(5), 2971–2984. <https://doi.org/10.5194/acp-24-2971-2024>
- 713 Mochida, M., & Kawamura, K. (2004). Hygroscopic properties of levoglucosan and related  
714 organic compounds characteristic to biomass burning aerosol particles. *Journal of  
715 Geophysical Research: Atmospheres*, 109(D21), 2004JD004962.  
716 <https://doi.org/10.1029/2004JD004962>
- 717 Nadler, K. A., Kim, P., Huang, D.-L., Xiong, W., & Continetti, R. E. (2019). Water diffusion  
718 measurements of single charged aerosols using H<sub>2</sub>O/D<sub>2</sub>O isotope exchange and Raman  
719 spectroscopy in an electrodynamic balance. *Physical Chemistry Chemical Physics*, 21(27),  
720 15062–15071. <https://doi.org/10.1039/C8CP07052K>
- 721 Nenes, A., Pandis, S. N., & Pilinis, C. (1998). *ISORROPIA: A New Thermodynamic Equilibrium  
722 Model for Multiphase Multicomponent Inorganic Aerosols*. *Aquatic Geochemicals* 4, 123–  
723 152.
- 724 Padró, L. T., Moore, R. H., Zhang, X., Rastogi, N., Weber, R. J., & Nenes, A. (2012). Mixing state  
725 and compositional effects on CCN activity and droplet growth kinetics of size-resolved  
726 CCN in an urban environment. *Atmospheric Chemistry and Physics*, 12(21), 10239–10255.  
727 <https://doi.org/10.5194/acp-12-10239-2012>
- 728 Peng, C., Chen, L., & Tang, M. (2022). A database for deliquescence and efflorescence relative  
729 humidities of compounds with atmospheric relevance. *Fundamental Research*, 2(4), 578–  
730 587. <https://doi.org/10.1016/j.fmre.2021.11.021>
- 731 Peng, C., Chow, A. H. L., & Chan, C. K. (2001). Hygroscopic Study of Glucose, Citric Acid, and  
732 Sorbitol Using an Electrodynamic Balance: Comparison with UNIFAC Predictions.  
733 *Aerosol Science and Technology*, 35(3), 753–758.  
734 <https://doi.org/10.1080/02786820152546798>



- 735 Peng, C., Jing, B., Guo, Y.-C., Zhang, Y.-H., & Ge, M.-F. (2016). Hygroscopic Behavior of  
736 Multicomponent Aerosols Involving NaCl and Dicarboxylic Acids. *The Journal of*  
737 *Physical Chemistry A*, 120(7), 1029–1038. <https://doi.org/10.1021/acs.jpca.5b09373>
- 738 Pope, F. D., Dennis-Smith, B. J., Griffiths, P. T., Clegg, S. L., & Cox, R. A. (2010). Studies of  
739 Single Aerosol Particles Containing Malonic Acid, Glutaric Acid, and Their Mixtures with  
740 Sodium Chloride. I. Hygroscopic Growth. *The Journal of Physical Chemistry A*, 114(16),  
741 5335–5341. <https://doi.org/10.1021/jp100059k>
- 742 Prenni, A. J., DeMott, P. J., Kreidenweis, S. M., Sherman, D. E., Russell, L. M., & Ming, Y.  
743 (2001). The Effects of Low Molecular Weight Dicarboxylic Acids on Cloud Formation.  
744 *The Journal of Physical Chemistry A*, 105(50), 11240–11248.  
745 <https://doi.org/10.1021/jp012427d>
- 746 Qu, W., Zhang, X., Wang, Y., & Fu, G. (2020). Atmospheric visibility variation over global land  
747 surface during 1973–2012: Influence of meteorological factors and effect of aerosol, cloud  
748 on ABL evolution. *Atmospheric Pollution Research*, 11(4), 730–743.  
749 <https://doi.org/10.1016/j.apr.2020.01.002>
- 750 Reich, O., Gleichweit, M. J., David, G., Leemann, N., & Signorell, R. (2023). Hygroscopic growth  
751 of single atmospheric sea salt aerosol particles from mass measurement in an optical trap.  
752 *Environmental Science: Atmospheres*, 3(4), 695–707.  
753 <https://doi.org/10.1039/D2EA00129B>
- 754 Saxena, P., Hildemann, L. M., McMurry, P. H., and Seinfeld, J. H.: Organics alter hygroscopic  
755 behavior of atmospheric particles, *J. Geophys. Res.*, 100D, 18 755–18 770, 1995
- 756 Shearman, R.W. and Menzies, A.W.C. (1937) The Solubilities of Potassium Chloride in  
757 Deuterium Water and in Ordinary Water from 0 to 180<sup>0</sup>. *J. Am. Chem. Soc.*, 59: 185.
- 758 Sjogren, S., Gysel, M., Weingartner, E., Baltensperger, U., Cubison, M. J., Coe, H., Zardini, A.  
759 A., Marcolli, C., Krieger, U. K., & Peter, T. (2007). Hygroscopic growth and water uptake  
760 kinetics of two-phase aerosol particles consisting of ammonium sulfate, adipic and humic  
761 acid mixtures. *Journal of Aerosol Science*, 38(2), 157–171.  
762 <https://doi.org/10.1016/j.jaerosci.2006.11.005>



- 763 Steimer, S. S., Krieger, U. K., Te, Y.-F., Lienhard, D. M., Huisman, A. J., Ammann, M., & Peter,  
764 T. (2015). *Electrodynamic balance measurements of thermodynamic, kinetic, and optical*  
765 *aerosol properties inaccessible to bulk methods*. <https://doi.org/10.5194/amtd-8-689-2015>
- 766 Tang, I. N., & Munkelwitz, H. R. (1991). Simultaneous Determination of Refractive Index and  
767 Density of an Evaporating Aqueous Solution Droplet. *Aerosol Science and Technology*,  
768 *15*(3), 201–207. <https://doi.org/10.1080/02786829108959527>
- 769 Topping, D., Barley, M., Bane, M. K., Higham, N., Aumont, B., Dingle, N., & McFiggans, G.  
770 (2016). UManSysProp v1.0: An online and open-source facility for molecular property  
771 prediction and atmospheric aerosol calculations. *Geoscientific Model Development*, *9*(2),  
772 899–914. <https://doi.org/10.5194/gmd-9-899-2016>
- 773 Wang, J., Cubison, M. J., Aiken, A. C., Jimenez, J. L., & Collins, D. R. (2010). The importance of  
774 aerosol mixing state and size-resolved composition on CCN concentration and the variation  
775 of the importance with atmospheric aging of aerosols. *Atmospheric Chemistry and Physics*,  
776 *10*(15), 7267–7283. <https://doi.org/10.5194/acp-10-7267-2010>
- 777 Wang, K., Huang, R.-J., Brüggemann, M., Zhang, Y., Yang, L., Ni, H., Guo, J., Wang, M., Han,  
778 J., Bilde, M., Glasius, M., & Hoffmann, T. (2021). Urban organic aerosol composition in  
779 eastern China differs from north to south: Molecular insight from a liquid chromatography–  
780 mass spectrometry (Orbitrap) study. *Atmospheric Chemistry and Physics*, *21*(11), 9089–  
781 9104. <https://doi.org/10.5194/acp-21-9089-2021>
- 782 Wang, X., Shi, Q., Zhao, Y., Wang, X., & Zheng, Y. (2013). MOISTURE ADSORPTION  
783 ISOTHERMS AND HEAT OF SORPTION OF *AGARICUS BISPORUS*: ADSORPTION  
784 ISOTHERMS OF *AGARICUS BISPORUS*. *Journal of Food Processing and Preservation*,  
785 *37*(4), 299–305. <https://doi.org/10.1111/j.1745-4549.2011.00649.x>
- 786 Wexler, A. and Hasegawa, S., 1954. Relative Humidity-Temperature Relationships of Some  
787 Saturated Salt Solutions in the Temperature Range 0°C to 50°C. *Journal of Research of the*  
788 *National Bureau of Standards*, *53*, 19-26. <https://doi.org/10.6028/jres.053.003>
- 789 Wexler, A. S., & Seinfeld, J. H. (1991). Second-generation inorganic aerosol model. *Atmospheric*  
790 *Environment. Part A. General Topics*, *25*(12), 2731–2748. [https://doi.org/10.1016/0960-](https://doi.org/10.1016/0960-1686(91)90203-J)  
791 [1686\(91\)90203-J](https://doi.org/10.1016/0960-1686(91)90203-J)





- 792 Zamora, I. R., & Jacobson, M. Z. (2013). Measuring and modeling the hygroscopic growth of two  
793 humic substances in mixed aerosol particles of atmospheric relevance. *Atmospheric*  
794 *Chemistry and Physics*, 13(17), 8973–8989. <https://doi.org/10.5194/acp-13-8973-2013>
- 795 Zamora, I. R., Tabazadeh, A., Golden, D. M., & Jacobson, M. Z. (2011). Hygroscopic growth of  
796 common organic aerosol solutes, including humic substances, as derived from water  
797 activity measurements: WATER ACTIVITY OF ORGANIC AEROSOLS. *Journal of*  
798 *Geophysical Research: Atmospheres*, 116(D23), n/a-n/a.  
799 <https://doi.org/10.1029/2011JD016067>
- 800 Zieger, P., Väisänen, O., Corbin, J. C., Partridge, D. G., Bastelberger, S., Mousavi-Fard, M.,  
801 Rosati, B., Gysel, M., Krieger, U. K., Leck, C., Nenes, A., Riipinen, I., Virtanen, A., &  
802 Salter, M. E. (2017). Revising the hygroscopicity of inorganic sea salt particles. *Nature*  
803 *Communications*, 8(1), 15883. <https://doi.org/10.1038/ncomms15883>
- 804 Zuend, A., Marcolli, C., Peter, T., & Seinfeld, J. H. (2010). Computation of liquid-liquid equilibria  
805 and phase stabilities: Implications for RH-dependent gas/particle partitioning of organic-  
806 inorganic aerosols. *Atmospheric Chemistry and Physics*, 10(16), 7795–7820.  
807 <https://doi.org/10.5194/acp-10-7795-2010>  
808